Materials and Design 39 (2012) 285–293

Contents lists available at SciVerse ScienceDirect

Materials and Design

journal homepage: www.elsevier.com/locate/matdes

Laser welding of TiNi shape memory alloy and stainless steel using Ni interlayer

H.M. Li [a], D.Q. Sun [a,*], X.L. Cai [b], P. Dong [a], W.Q. Wang [a]

[a] Key Laboratory of Automobile Materials, Ministry of Education, Department of Materials Science and Engineering, Jilin University, No. 5988 Renmin Street, Changchun 130025, PR China
[b] State Key Laboratory of Rare Earth Resources Utilization, Changchun Institute of Applied Chemistry, Chinese Academy of Sciences, No. 5625 Renmin Street, Changchun 130022, PR China

ARTICLE INFO

Article history:
Received 28 September 2011
Accepted 16 February 2012
Available online 6 March 2012

Keywords:
A. Intermetallics
D. Welding
F. Microstructure

ABSTRACT

Laser welding of TiNi shape memory alloy wire to stainless steel wire using Ni interlayer was investigated. The results indicated that the Ni interlayer thickness had great effects on the chemical composition, microstructure, gas-pore susceptibility and mechanical properties of laser-welded joints. With an increase of Ni interlayer thickness, the weld Ni content increased and the joint properties increased due to decreasing brittle intermetallic compounds ($TiFe_2$ and $TiCr_2$). The joint fracture occurred in the fusion zone with a brittle intermetallic compound layer. The tensile strength and elongation of the joints reached the maximum values (372 MPa and 4.4%) when weld Ni content was 47.25 wt.%. Further increasing weld Ni content resulted in decreasing the joint properties because of forming more $TiNi_3$ phase, gas-pores and shrinkage cavities in the weld metals. It is necessary to select suitable Ni interlayer thickness (weld composition) for improving the mechanical properties of laser-welded joints.

1. Introduction

TiNi shape memory alloy is a new kind of function material, which possesses special shape memory effect and superelasticity as well as excellent erosion resistance and good biocompatibility [1,2]. It has broad application prospects in many fields, such as aviation and space-flight, atomic energy, ocean development, mechanic–electronic and medical device [3–6]. As is well known, successful applications of any advanced material not only hinge on its inherent properties, but also depend on the development of joining technologies (joining of TiNi alloy to itself or other materials). At present, successful fusion welding, particularly laser welding, of TiNi alloy to itself has been well established [7–10]. However, very few studies have been conducted on welding TiNi alloy to other materials, such as stainless steel which is widely used for medical devices owing to its mechanical properties, workability, low cost and corrosion resistance [11]. The joining of TiNi alloy to stainless steel would be a desirable material combination for many applications. But, large differences in physical and chemical properties between the two materials make the dissimilar welding complex and difficult. Brittle intermetallic compounds such as $TiFe_2$ and $TiCr_2$ were formed in joints when TiNi alloy was welded to stainless steel directly, which are reasons for the low tensile strength and the brittle fracture of the joints [12–15]. It has been reported that the weld microstructures and joint properties can be improved by using AgCu interlayer in transient liquid phase diffusion bonding (TLP-DB) [16–18], silver based fillers in laser-brazing [19,20] and brazing [21], and Ni interlayer in friction welding [22]. In the processes mentioned above, the joints are formed without large-scale melting of the base metals (TiNi alloy and stainless steel). The absence of liquid prevents or minimizes the formation of brittle intermetallic compounds. These processes, however, are usually limited to particular joint geometries and dimensions. From an engineering point of view, the fusion welding is more attractive due to its more wide applications. Hall reported that the brittle intermetallic phase, $TiFe_2$, made the resulting weld equally brittle and laser welding using Ni filler metal could greatly improve the mechanical performance of TiNi-stainless steel fusion welds [23]. But, up to now, the weldability characteristics (such as microstructures, gas-pores and cracks) of TiNi alloy to stainless steel and effects of Ni filler metal have not been fully understood. Therefore, further research and development efforts are required.

The present work investigates effects of Ni interlayer thickness on the chemical composition, microstructure, gas-pore susceptibility and mechanical properties of laser-welded joints. Its objective was to evaluate the weldability of TiNi alloy to stainless steel and to provide some foundation for improving the mechanical properties of the dissimilar joints.

2. Experimental procedure

2.1. Materials and sample preparation

TiNi shape memory alloy (TiNi SMA) wires (Ti–49.8 at.%Ni) and AISI304 stainless steel (SS) wires with the composition of Fe–

* Corresponding author. Tel./fax: +86 431 85094687.
E-mail addresses: sundq@jlu.edu.cn, psdq@sina.com (D.Q. Sun).

0261-3069/$ - see front matter © 2012 Elsevier Ltd. All rights reserved.
doi:10.1016/j.matdes.2012.02.031

Table 1
Mechanical properties of TiNi alloy and stainless steel wire.

Materials	Tensile strength (MPa)	Yield strength (MPa)	Elongation (%)
TiNi alloy	1030 ± 20	255	15–18
Stainless steel	1870 ± 30	–	3.8–4.2

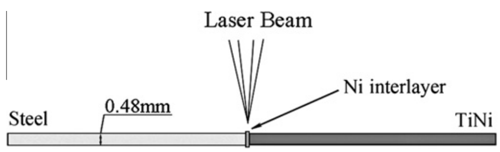

Fig. 1. Schematic diagram of laser-welded TiNi SMA and stainless steel with Ni interlayer.

0.05C–0.8Si–1.9Mn–17.5Cr–9Ni (wt.%) were used in this investigation. The dimension of the wires was 30 mm (length) × 0.64 mm (width) × 0.48 mm (thickness). Their mechanical properties are shown in Table 1. The pure nickel foil (10–100 μm thick and 99.95% purity) was used as interlayer material. Before welding, the oxide layer on the wires was removed by grinding, and then ultrasonically cleaned in an acetone bath. The nickel foil was cleaned in acetone and dried in air.

2.2. Laser welding

The TiNi SMA–Ni–SS assembly was kept in contact in a self-constructed fixture, as shown in Fig. 1. Welding process was performed using a Nd:YAG laser welding system (Type JHM-1GY-300B). The samples were welded with a single pulse, at the input energy of 7.20 J, the pulse duration of 10 ms, the laser beam diameter of 0.3 mm and the focus distance of 55 mm [24]. During laser welding, Ar shield gas prevented N_2, O_2 and H_2 from penetrating into the weld zone and reducing the joint properties. The addition of Ni was changed by changing Ni interlayer thickness.

2.3. Metallography

The laser-welded joint samples were polished and then etched with 5 mL HF + 20 mL HNO3 + 25 mL H_2O solution. The macrostructure of joints was observed by Confocal Laser Scanning Microscope (CLSM, OLYMPUS OSL3000). The chemical composition, microstructure and fracture surface morphology of the joints were examined using scanning electron microscopy (SEM, EVO18) equipped with energy dispersive X-ray spectroscopy (EDS, Link-ISIS). The phase identification was done in the central area of weld zone (diameter of 500 μm) by micro X-ray diffraction (M-XRD, D8 Discover with GADDS). A further microstructure analysis was carried out using transmission electron microscopy (TEM, JEM-2100F) with selected area electron diffraction (SAED). TEM specimens were prepared by hand-grinding to 30 μm, and then stuck to a copper ring by special glue followed by ion milling (dual guns operating at 5 kV/1.8 mK per gun, with gun-to-specimen angles of 15°). These specimens were examined at accelerating voltages of 200 kV to produce bright-field and dark-field images as well as selected area and micro-diffraction patterns.

2.4. Test of mechanical properties

All mechanical property tests were conducted at room temperature. The microhardness was performed on the laser-welded joints, according to standard ASTM E384 [25], using a Vickers hardness tester (MH-3 Everone) with a load of 200 gf and a dwell time of 15 s. Additional hardness tests were done on the fusion zones and somewhere has special structure. The average hardness value was determined by 10 test point measurements. Static tensile tests were carried out by means of the material test systems (MTS 810). Due to the limited length of the specimen, the design of non-standard specimen was performed with reference to ASTM E8 [26]. The displacement velocity of tensile specimen was 0.2 mm/min and the gauge length was 40 mm.

3. Results and discussion

3.1. Joint microstructures

The TiNi alloy was laser welded to stainless steel using 10–100 μm thick Ni interlayers, respectively. Fig. 2 shows the macroscopic metallographic images and EDS line scan results of laser-welded joints. The dissimilar metal joints consisted of the weld zone (WZ), heat-affected zones (HAZs) and base metals (BMs). Full-penetration weld metals could be distinguished from the base metals easily. All the weld zones exhibited swirling characteristics caused by the flow of liquid metal in laser welding pools. The EDS line scan analysis across the joints indicated that the distribution of Ti, Ni, Fe and Cr elements varied significantly over the WZs. From stainless steel side to TiNi alloy side, the concentration of Fe and Cr decreased and that of Ti and Ni had an increased tendency. As can be seen, the WZ can be divided into three regions by color, the dark region, gray region and white region. The dark region was rich in Ti and Ni with relatively low concentration of Fe and Cr, the white region had higher concentration of Fe and Cr than the dark region, and the compositions of the gray region were between those of dark region and white region. These results suggested that the distribution of elements and microstructures was non-uniform for the laser weld metals. It is well known that laser welding is characterized by extremely high heating and cooling rates, which affect the homogenization process of chemical composition in weld pool, hence resulting in non-uniform microstructures.

The EDS analysis revealed that the Ni interlayer thickness had a great effect on the chemical composition of laser welds. Fig. 3 shows weld Ti, Ni, Fe and Cr contents as a function of Ni interlayer thickness. The thicker the Ni interlayer, the richer Ni is and the lesser Ti, Fe and Cr in the WZs are. Increasing the Ni interlayer thickness from 10 μm to 100 μm, the weld Ni content increased from 27.84 wt.% to 66.41 wt.%, and weld Ti, Fe and Cr contents decreased from 19.61 wt.%, 40.43 wt.% and 12.12 wt.% to 8.65 wt.%, 19.65 wt.% and 5.29 wt.%, respectively. It is attributed to the more addition of Ni and the reduction of the fusion ratio of base metals (TiNi alloy and stainless steel). It is favorable to add Ni for minimizing the formation of brittle intermetallic compounds ($TiFe_2$ and $TiCr_2$).

The authors described laser-brazing of TiNi alloy to stainless steel using silver based fillers. The weld microstructures mainly depended on filler compositions [20]. For plasma welding of TiNi alloy to stainless steel with a Ni rich filler wire, the weld matrix phase is a mixture of Ti, Ni and Fe while the eutectic phase is a Ni-rich phase [12]. Hall reported that a large amount of brittle $TiFe_2$, which is a primary crystal in the Fe–Ni–Ti ternary phase diagram, was formed with $TiNi_3$ as a eutectic phase in the laser weld, and suggested that future analysis would include more thorough characterization of the weld metallurgy and phase identification [23]. In this investigation, it was found that the phase composition of the laser weld was very complicated and the Ni interlayer thickness had great effects on weld microstructures.

Figs. 4 and 5 show SEM microstructures and XRD patterns of welds made with 10–100 μm thick Ni interlayers, respectively. When the Ni interlayer thickness was in the range of 10–60 μm,